JACS
JOURNAL OF THE AMERICAN CHEMICAL SOCIETY
Article
pubs.acs.org/JACS

Radical-Involved Photosynthesis of AuCN Oligomers from Au Nanoparticles and Acetonitrile

Renhong Li,[†] Hisayoshi Kobayashi,[‡] Jiawei Tong,[†,∥] Xiaoqing Yan,[†] Yu Tang,[†] Shihui Zou,[†] Jiabin Jin,[†] Wuzhong Yi,[†] and Jie Fan*[,†]

[†]Key Lab of Applied Chemistry of Zhejiang Province, Department of Chemistry, Zhejiang University, Hangzhou, Zhejiang Province 310027, China

[‡]Department of Chemistry and Materials Technology, Kyoto Institute of Technology, Matsugasaki, Sakyo-ku, Kyoto, Japan

Supporting Information

ABSTRACT: We show here the first radical route for the direct photosynthesis of AuCN oligomers with different sizes and shapes, as evidenced by TEM observations, from an Au nanoparticle/benzaldehyde/CH_3CN ternary system in air under UV-light irradiation. This photochemical route is green, mild, and universal, which makes itself distinguishable from the common cyanidation process. Several elementary reaction steps, including the strong C−C bond dissociation of CH_3CN and subsequent •CN radical addition to Au, have been suggested to be critical in the formation of AuCN oligomers based on the identification of •CN radical by *in situ* EPR and the radical trapping technique, and other reaction products by GC-MS and ^{1}H NMR, and DFT calculations. The resulting solid-state AuCN oligomers exhibit unique spectroscopic characters that may be a result of the shorter Au−Au distances (namely, aurophilicity) and/or special polymer-like structures as compared with gold cyanide derivatives in the aqueous phase. The nanosized AuCN oligomers supported on mesoporous silica showed relatively good catalytic activity on the homogeneous annulation of salicylaldehyde with phenylacetylene to afford isoflavanones employing PBu_3 as the cocatalyst under moderate conditions, which also serves as evidence for the successful production of AuCN oligomers.

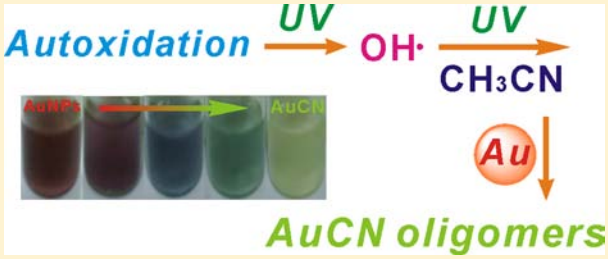

1. INTRODUCTION

As one of the noble metals, gold has a distinct position among the elements in the Periodic Table.[1] Despite the fact that it is one of the most inert metals, gold actually has a rich coordination and organometallic chemistry.[2,3] AuCN, a gold complex that is stable in air and water with a stability constant as large as 10^{37} M^{-2} due to the strong relativistic effects in gold,[4] has a wide variety of applications in the fields of, for example, adsorption,[5] catalysis,[6] surface enhanced Raman scattering (SERS),[7] sensors,[8] and photoluminescence.[9] The conventional preparation of AuCN from Au requires a two-step cyanidation process. The first step is the conversion of gold into a water-soluble coordination complex ($Au(CN)_2^-$) in the presence of cyanide ions and molecular oxygen. The relevant chemical reaction is described as the "*Elsner Equation*":

$$4Au + 8[CN]^- + 2H_2O + O_2 \rightarrow 4[Au(CN)_2]^- + 4[OH]^- \quad (1)$$

Then the $Au(CN)_2^-$ complex can be transformed into AuCN solid. To achieve this, concentrated acid (usually HCl) is required to remove the counterions (e.g., Na^+ or K^+):

$$4[Au(CN)_2]^- + HCl \rightarrow AuCN + Cl^- + HCN \quad (2)$$

However, due to the highly poisonous nature of cyanide ions, the above cyanidation process is controversial and its usage is forbidden in many countries and territories. In the wake of the increasing concern about the environment, developing a one-pot and green synthetic strategy to make AuCN solid from metallic Au is very desirable but remains a blank and unexplored realm.

Herein, for the first time, we report a photoassisted route that allows AuCN nanoparticles (NPs) to be oligomerized on various supports using acetonitrile (MeCN) and AuNPs as raw materials. This method has been demonstrated to be green, mild, and universal. Importantly, we propose that the syntheses involve three crucial elementary steps based on the identification of •CN radicals and DFT calculations: (1) The autoxidation of aromatic molecules with molecular oxygen under UV-light irradiation leads to the generation of reactive oxygen species (ROS), mainly •OH radicals. (2) The ROS abstracts a H atom from MeCN to produce $•CH_2CN$ radicals; the resultant $•CH_2CN$ radicals interact with MeCN molecules that break the strong C−C bonds of MeCN to release •CN radicals and CH_3CH_2CN. Meanwhile, a putative AuOH intermediate may also be formed at this stage. (3) Finally, in addition to the reaction between CH_3CH_2CN and AuOH to produce CH_3CH_2OH and AuCN, the reaction of •CN radicals with surface gold atoms results in the formation and radical-

Received: May 29, 2012
Published: October 14, 2012

   dx.doi.org/10.1021/ja305198p | J. Am. Chem. Soc. 2012, 134, 18286−18294

induced oligomerization of AuCN inorganic polymers on the supports.

During the whole photosynthesis, the ROS-assisted cleavage of the C−C bond of MeCN and the sequential direct •CN radical cyanidation of AuNPs seem to be of potential significance. Actually, the former reaction is difficult to realize due to the particularly strong C−C bond energy of MeCN (133 kcal/mol) compared with the alkane C−C bond energy (ca. 83 kcal/mol), such that it is of potential benefit to the synthesis of complex organic molecules from organonitriles.[10−15] The latter radical reaction leads to the construction of Au−C and Au−N bonds with strong covalent multiple-bond character,[4] thus offering a radical mean to establish a new bridge between transitional-metal based inorganic and organometallic chemistry, which completely differs from the common cyanidation processes involving toxic cyanide ions.

To demonstrate the versatility of the present photosynthetic route as well as the existence of AuCN species, AuCN solids on different supports were synthesized and subsequently applied for a typical C−C bond formation reaction, that is, the annulation of salicylaldehyde with phenylacetylene to afford isoflavanones under moderate conditions.[16,17] Recent progress in the area of catalytic C−C bond formation has been reported using homogeneous gold catalysts such as $AuBr_3$ or AuCl,[18,19] but relatively few publications have appeared employing AuCN as the main catalytic species.[17] One possible reason is that the toxicity involved in the conventional cyanidation process arrests the intention to use AuCN as a catalyst. In the present investigation, it is confirmed that AuCN indeed participated in the catalytic annulation process, where mesoporous silica loaded with AuCN oligomers gave the highest yield of the product among tested catalysts.

2. EXPERIMENTAL SECTION

2.1. Synthesis of $AuPPh_3Cl$. $AuPPh_3Cl$ is synthesized from $HAuCl_4{\cdot}4H_2O$ and PPh_3 precursors. In a typical synthesis, 1 g of $HAuCl_4{\cdot}4H_2O$ is added into 35 mL of ethanol aqueous solvent ($V_{ethanol}$:V_{H_2O} = 33:2). Meanwhile, 1.364 g of PPh_3 solid is added into 50 mL of ethanol aqueous solvent ($V_{ethanol}$:V_{H_2O} = 48:2). The two solvents are then mixed together to afford a yellow suspension. After stirring for 2 min, the visual color of the suspension is changed from yellow to white, meaning $AuPPh_3Cl$ is formed. $AuPPh_3Cl$ solid is collected and preserved after washing with ethyl ether several times.

2.2. Synthesis of Supported AuNPs. A 100 mg portion of as-synthesized $AuPPh_3Cl$ was mixed with 400 μL of dodecanethiol in 20 mL of benzene to form a clear solution, to which 84 mg of $NaBH_4$ was then added in one portion. The mixture was heated with stirring at 328 K for 6 h before the reaction system was cooled to room temperature. AuNPs were precipitated out from the reaction mixture as black solid powders by addition of 20 mL of ethanol. The precipitate was separated by centrifuge, washed with ethanol, and dried naturally. AuNPs was loaded into various supports by a colloid deposition method. A desired amount of AuNPs was dissolved in 25 mL of chloroform. To this solution, a desired amount of supports was added. After 30 min of stirring, the solid product was centrifuged and dried in air. The supported AuNPs were calcined at 823 K for 5 h before photoreaction. The detailed synthesis of silica supports (FDU-12 and SiO_2MS) is available in the Supporting Information.

2.3. Photosynthesis of AuCN. Supported AuCN was carried out with 40 mg of 5.0 wt % AuNPs/support suspended in 4 mL of acetonitrile solution containing 100 μmol of benzaldehyde (or benzyl alcohol) in air under stirring. Side-irradiation by a 300 W high-pressure mercury lamp was used to initiate the photoreaction. After 4−6 h of reaction, the solid product was obtained by centrifuging and drying in air at 363 K overnight.

2.4. Material Characterization. Wide-angle XRD patterns were recorded on a Bruker D8 diffractometer using Cu Kα radiation. TEM images were recorded on a JEOL JEM-1230 instrument operated at 100 kV. The sample was embedded in epoxy resin and then microtomed into sub-100 nm ultrathin film at room temperature. These thin film samples floating on water or other solvents were collected by copper mesh with a polymer microgrid for TEM imaging. Solid UV/vis adsorption spectra were measured with a Shimadzu UV-2450 spectrophotometer in the diffuse reflectance mode. XPS measurements were performed in a VG Scientific ESCALAB Mark II spectrometer equipped with two ultrahigh vacuum (UHV) chambers. All binding energies were referenced to the C1s peak at 284.8 eV of the surface adventitious carbon. Laser Raman spectra were collected under ambient conditions using an HR LabRaman 800 system equipped with a CCD detector. A green laser beam (λ = 514.5 nm) was used for excitation. ^{1}H NMR spectra were recorded at 400 MHz using TMS as the internal standard (0 ppm) for $CDCl_3$. X-band EPR signals were recorded at ambient temperature on a Bruker EPR A-300 spectrometer. The settings for the EPR spectrometer were as follows: center field, 3511.39 G; sweep width, 100 G; microwave frequency, 9.86 G; modulation frequency, 100 kHz; power, 101 mW; conversion time, 10 ms. 5,5-Dimethyl-pyrroline-*N*-oxide (DMPO) and *N*-*t*-butyl-α-nitrone (PBN) spin-trapping reagents and other chemicals were purchased from Sigma-Aldrich Chemical Co. and used without further purification. Detailed EPR processes and control experiments are available in the Supporting Information.

2.5. AuCN-Catalyzed Organic Synthesis. In a typical synthesis, 5 mL of salicylaldehyde, 0.11 mL of phenylacetylene, 29.7 mg of supported AuCN (5.0 wt %), and 0.083 mL of PBu_3 (1.0 M in distilled toluene) were stirred in a sealed reactor at 403 K under nitrogen for 36 h. The reaction mixture was cooled to room temperature, and the solvent was evaporated in vacuo. The residue was purified by flash-column chromatogrphy on silica gel with the appropriate mixture of petroleum ether and ethyl acetate to give needle-like yellow isoflavanone crystal. Its spectral data are consistent with those reported in the literature.[17] A doublet (J = 7.2 Hz) is observed in the ^{1}H NMR spectrum at δ = 4.68 ppm for the two hydrogen atoms α to the oxygen atom of the ether group, and a triplet (J = 7.2 Hz) is observed at δ = 4.02 ppm for the hydrogen atom α to the carbonyl group.

3. RESULTS AND DISCUSSION

3.1. Characterizations. AuNPs with a uniform size of 3.3 ± 0.5 nm were prepared according to our previous method (Figure S1 in the Supporting Information).[20] They were readily adsorbed onto various supports by colloid deposition, followed by high-temperature thermal treatment. In a typical synthesis of AuCN materials, the supported AuNPs were transferred into a MeCN solution containing a certain amount of benzaldehyde for UV-light irradiation (λ > 300 nm) at room temperature (298 K). With the increase of irradiation time, the visual color of the suspension is changed from wine red to marroon, then to celadon, and finally to pale green (inset photographs of Figure 1a). It is obvious from the X-ray powder diffraction (XRD) patterns and indexing that AuNPs have been completely transformed into crystalline AuCN after the photoreaction (Figure 1a). The XRD pattern corresponds to a hexagonal compound with the space group *P6mm* (lattice parameters: a = b = 3.395, and c = 5.080 Å). In addition, as compared with AuNPs, the Au 4f X-ray photoelectron spectroscopy (XPS) binding energies of AuCN samples shift from 87.7 to 88.7 eV for Au $4f_{5/2}$ signals and 84.1 to 85.1 eV for Au $4f_{7/2}$ signals (Figure 1b), respectively. The 1.0 eV red-shift of the Au 4f peaks as well as the appearance of the N 1s peak (Figure 1b, inset) further confirm the formation of AuCN species.

Although AuCN solid has been known for centuries, much of its photophysical and photochemical properties remain unclear

dx.doi.org/10.1021/ja305198p | J. Am. Chem. Soc. 2012, 134, 18286−18294

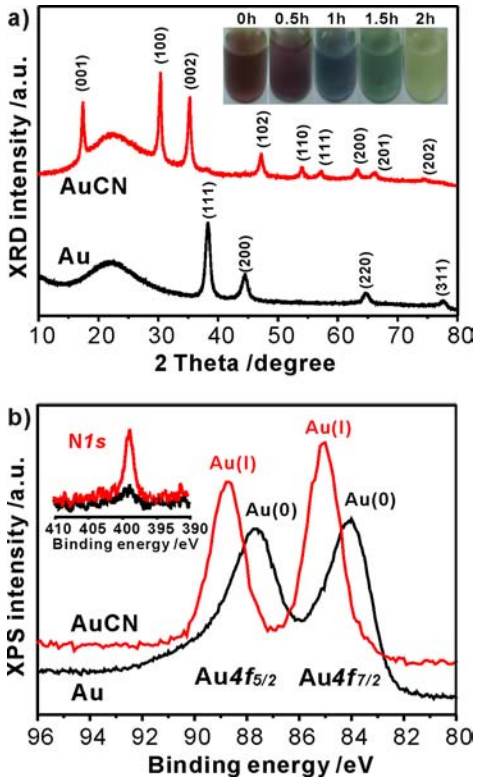

Figure 1. (a) XRD patterns and photographs of time-dependent color evolution (inset) and (b) Au 4f and N 1s (inset) XPS peaks.

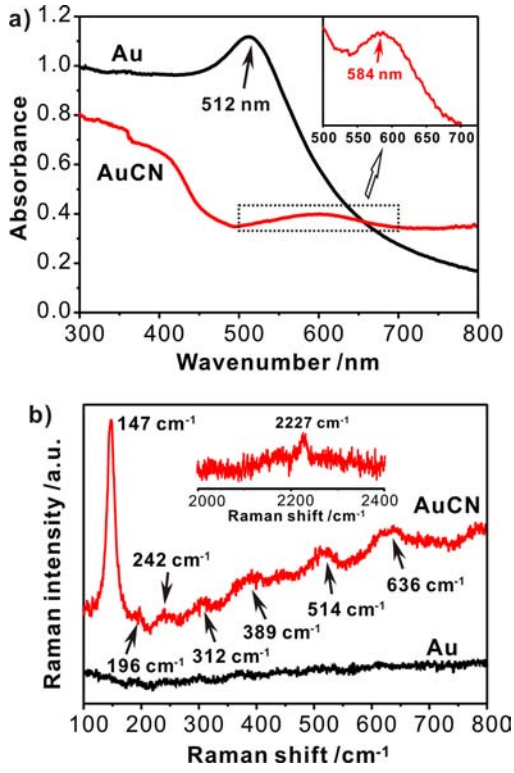

Figure 2. (a) UV−vis absorbance and (b) Raman spectra of AuNPs and AuCN NPs loaded on silica supports.

especially at the nanoscale. Consequently, solid UV−vis and laser Raman spectroscopy are employed to determine the spectroscopic properties of AuCN samples. As shown in Figure 2a, an unexpected broad absorption band covers the entire visible region with a local maximum at λ = 584 nm (inset) appearing for AuCN, which is much different from the localized surface plasmon resonance (LSPR) at λ = 512 nm for AuNPs. Usually only UV absorption is possible for analogous Au(I) cyanides due to monomer metal-to-ligand charge transfer (MLCT).[21] However, it has been clarified that the reduction in the metal−metal distance in the oligomers will lead to a smaller HOMO−LUMO energy gap, and that the Au−Au antibonding and bonding characters give rise to the concomitant destabilization of the HOMOs and the stabilization of the LUMOs, respectively.[21,22] While most previous studies focused on the solution phase,[21] the present solid-state AuCN oligomers with substantially reduced Au−Au distance may be responsible for its visible absorption band.

For Raman analysis, pristine AuNPs exhibit no Raman scattering in the range 100−800 cm^{-1}; however, an intense oscillation mode at 147 cm^{-1} arises for AuCN (Figure 2b). To date, seldom reports contain data for the low-frequency region below 200 cm^{-1} for AuCN and its derivatives.[7] The new strong mode displayed here is possibly attributed to the Au—Au stretch vibrational frequency, ν(Au—Au), due to the 5dσ*−6pσ electronic transition.[23] The other three neighboring signals at 196, 242, and 312 cm^{-1} could thus be designated as 2ν(Au—Au), 3ν(Au—Au), and 4ν(Au—Au), respectively. In addition to ν(Au—Au), the Raman signals at 389 cm^{-1} are tentatively assigned to the Au—CN bending motion, δ(Au—CN), 514 cm^{-1} to the Au—CN stretching mode, ν(Au—CN), 636 cm^{-1} to the Au—NC stretching mode, ν(Au—NC),[7] and 2227 cm^{-1} (inset) to the CN^- stretching motion, ν(C≡N). Notably, the obtained values are much larger than that of the similar assignments given in the literature,[7,24] which is supposed to be caused by the formation of solid AuCN oligomers with weaker Au—C and C≡N bond energy as compared with aqueous phase $KAu(CN)_2$ or $NaAu(CN)_2$ monomers.

3.2. Mechanism Exploration. The elucidation of the reaction mechanism is a very important issue of this work. It is amazing that even AuNPs are etched in the simple liquid including only aromatic molecules and MeCN under UV irradiation. Are cyanide ions, like other common cyanidation processes, present in the reaction system? To address this, we found that only CO_2 and O_2 are detected in the gas phase of the reaction system, and neither HCN nor other potentially harmful cyanide ions are detected in the liquid phase, demonstrating the green nature of our synthetic strategy. Therefore, there must be an alternative cyanide source for the formation of AuCN.

According to the control experiments, we found that UV-light, benzaldehyde (or benzyl alcohol), and molecular oxygen are all imperative factors for the successful synthesis of AuCN from AuNP/MeCN suspension (see the Supporting Information and control experiments therein). It is natural to expect that some radicals exist in our photoreaction system. We are aware of certain types of organic materials, such as unsaturated compounds with benzylic hydrogen, that are prone to undergo autoxidation that yields free radicals in the presence of oxygen and/or UV irradiation.[25] As a consequence, room-temperature electron paramagnetic resonance (EPR) spectroscopy and the spin trapping technique are primarily employed as an *in situ* analysis to detect potential radicals originated from the photochemical system. No EPR signals were observed in the solution containing DMPO spin trap reagent and MeCN in open air even under UV-light irradiation (Figure 3a, black line),

dx.doi.org/10.1021/ja305198p | J. Am. Chem. Soc. 2012, 134, 18286−18294

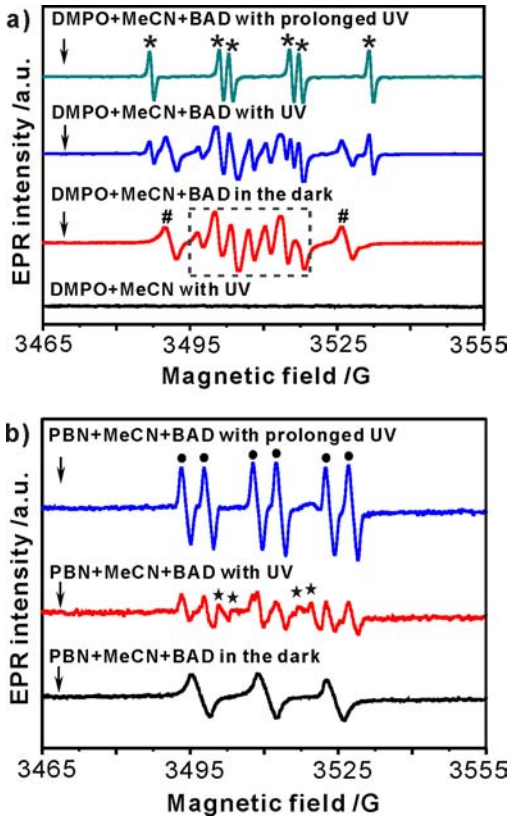

Figure 3. *In situ* EPR spectra of (a) DMPO and (b) PBN adducts recorded in the MeCN/BAD binary system at room temperature with/without UV-light irradiation (λ > 300 nm); herein, BAD represents benzaldehyde.

indicating that the C−C bond of MeCN is so strong that UV-light alone is unable to break it. It is intriguing to find that a seven-line signal (as indicated in the dashed square) designated to 5,5-dimethyl-2-pyrrolidone-*N*-oxyl species (DMPOX; hyperfine splitting constants: α_N = 6.98 G and α_H = 3.81 G)[26] along with two unknown peaks (with pound symbol) immediately appeared by addition of benzaldehyde (Figure 3a, red line). It is speculated that a sort of ROS, such as $O_2^{\bullet-}$, OH•, and •OOH, may be generated *via* benzaldehyde autoxidation, since under certain circumstances DMPOX can stem from the attack of free radicals (e.g., •ClO_2).[26] As a matter of fact, the two unresolved peaks are suggested to be parts of the quadruple DMPO−OH• adduct[27,28] ($\alpha_N = \alpha_H^{\beta}$ = 12.4 G) but overlapped and interfered by the stronger DMPOX signal. As soon as the onset of UV-light, a new six-line EPR signal (with asterisk) characteristic for the DMPO−•CN adduct[29] (α_N = 14.5 G, α_H^{β} = 22.4 G) was generated; meanwhile, the intensities of DMPOX and OH• radicals were decayed to a certain extent (Figure 3a, blue line). Continuous UV photoexcitation not only led to the enhancement of the DMPO−•CN adduct but also to the vanishing of the other two original radicals (Figure 3a, green line), implying that the production of •CN radicals from MeCN would consume some OH• radicals.

Another common spin trap agent, PBN, was used for double-checking the existence of ROS and •CN radicals. Consistent with the case of DMPO, a triplet peak (Figure 3b) perhaps for the oxidized state of PBN[30,31] (α_N = 13.5 G, g = 2.008) was observed under dark conditions, and a six-line spectrum (Figure 3b, black dots) of the PBN−•CN adduct (α_N = 14.6 G, α_H^{β} = 4.65 G)[32] accompanied with some low signals (with black stars) possibly attributed to the PBN−•OH adduct were also generated rapidly with incident UV-light. Meanwhile, the PBN−OH• adduct totally disappeared and the PBN−•CN adduct was progressively strengthened upon prolonged photoirradiation (Figure 3b, blue line). These results are in good agreement with the DMPO trapping experiments, unambiguously confirming that the photoassisted interaction between the ROS and MeCN molecules cleaves the strong C−C bond of MeCN to release •CN radicals.

We also recorded the DMPO adducts in the AuNP/MeCN/benzaldehyde ternary system at room temperature with/without UV-light irradiation (Figure 4). Interestingly, in

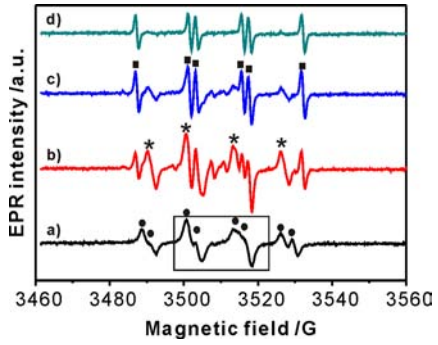

Figure 4. *In situ* EPR spectra of DMPO adducts recorded in the AuNP/MeCN/benzaldehyde ternary system at room temperature with/without UV-light irradiation (λ > 300 nm); in detail, (a) the suspension of AuNPs, DMPO, benzaldehyde, and MeCN under dark conditions, (b) the suspension of (a) once UV-light was on, (c and d) the suspension of (b) with prolonged UV irradiation.

contrast to the system without AuNPs, under dark conditions, the present ternary system exhibits an obvious six line signal (Figure 4a, black dots) which is ascribed to the peroxide radicals (such as $O_2^{\bullet-}$ or •OOH); meanwhile, the DMPOX signal is suppressed to a great extent (the black dots in the hollow rectangle). This may be a result of the change of chemical environment in the presence of AuNPs that interact strongly with MeCN molecules, dissolved molecular oxygen, and even DMPO itself. When UV-light set on, the DMPO−OH• adduct (Figure 4b, asterisk) and DMPO−•CN adduct (Figure 4c, black solid squares) were both emerged. The intensity of the DMPO−•CN adduct was increased, while the intensity of the DMPO−OH• adduct was degraded with prolonged light irradiation (Figure 4d). These results are consistent with the photochemical system without AuNPs. Prolonging the UV irradiation leads to a decrease of the DMPO−•CN signal (Figure 4d) due to the formation of AuCN. According to the EPR spin-trapping results, it is reasonable to conclude that •CN radicals are indeed generated and then are able to serve as a cyanide source in the photosynthesis of AuCN, which we will discuss later. In addition, the radical-involved character is also quite common in light-initiated reactions in nature.

In addition to the identification of the important reaction intermediates (e.g., •CN, ROS), the examination of the liquid as well as gas-phased products in the reaction system is also helpful for us to understand the reaction mechanism. Before doing so, it should bear in mind that UV-light-induced aerobic reaction often leads to a complete destroy of organic molecules due to its powerful photonic energy,[33] which makes the exact determination of organic products difficult and sometimes even

dx.doi.org/10.1021/ja305198p | J. Am. Chem. Soc. 2012, 134, 18286−18294

controversial. Nevertheless, gas chromatography (GC-TCD and GC-MS) and nuclear magnetic resonance (^{1}H NMR) analysis are still employed to examine the available products involving methyl and nitrile groups (Figure S2−S4 in the Supporting Information). As mentioned before, the green nature of our photoreaction system has been demonstrated, since only CO_2 and O_2 are detected in the gas phase, and neither HCN nor harmful cyanide ions are detected in the liquid phase. Interestingly, while no CH_3OH and negligible CH_3CH_2OH are present in the blank sample without AuNPs, a detectable amount of CH_3CH_2OH and CH_3CH_2CN are formed as two major byproducts in the AuNPs/MeCN suspension based on the ^{1}H NMR results.

In order to establish a possible reaction pathway to the formation of AuCN involving •CN radicals and ROS, the DFT calculations were carried out using the Gaussian 03W software with the B3LYP functional. The basis sets were LanL2DZ for Au and 6-311G(d,p) for others (Table 1). Herein, we

Table 1. Tentative Reaction Pathways to the Photosynthesis of AuCN from Au and MeCN[a]

Step 1:	$2CH_3CN + 2•OH \rightarrow 2•CH_2CN + 2H_2O$
Step 2:	$2CH_3CN + 2•CH_2CN \rightarrow 2•CN + 2CH_3CH_2CN$
Step 3:	$Au + •OH \rightarrow AuOH$
Step 4:	$CH_3CH_2CN + AuOH \rightarrow CH_3CH_2OH + AuCN$
Step 5:	$2Au + 2•CN \rightarrow 2AuCN$

[a]The reaction profiles for steps 1−5 were investigated by the DFT calculations. Steps 3 and 5 are a combination between species with odd electrons, and they proceed spontaneously. The reaction energies are −16.8 and −85.6 kcal/mol, respectively.

employed the •OH radical as a representative ROS to simplify the mechanism study. However, it seems reasonable that other types of free ROS have the ability to facilitate the photosynthesis of AuCN as well. Initially, we demonstrated the H atom abstraction from MeCN by the •OH radical, which produces $•CH_2CN$ and H_2O with very low activation energy (step 1 in Table 1 and Figure 5). The resulting $•CH_2CN$ reacts with another MeCN and produces the •CN radical by the following reaction (step 2 and Figure 6):

$$CH_3CN + •CH_2CN \rightarrow •[NCCH_3CH_2CN] \rightarrow •CN + CH_3CH_2CN \quad (3)$$

The reaction is endothermic by 46 kcal/mol with an activation energy of 64 kcal/mol. The reason why this type of reaction is conceived is that the $•CH_3$ radical was not detected at all. Then the next question is how the $-CH_3$ moiety from MeCN settles in CH_3CH_2OH without originating from CH_3OH. It is natural to suppose that CH_3CH_2OH is produced by the reaction between CH_3CH_2CN and OH• *via* radical transfer (i.e., $CH_3CH_2CN + OH• \rightarrow CH_3CH_2OH + •CN$), but the DFT calculation negates this route (Figure S5 in the Supporting Information). Scholz and co-workers have reported that OH• radicals in Fenton's reagent preferentially oxidize asperities on the gold surface.[34,35] Following this discovery, we hypothesize that AuOH intermediates might be formed on the surface of AuNPs under OH• radical attack (step 3). Indeed, by passing through AuOH, CH_3CH_2OH can be obtained energetically favorable at the expense of CH_3CH_2CN (step 4 and Figure S6 in the Supporting Information). This reaction is

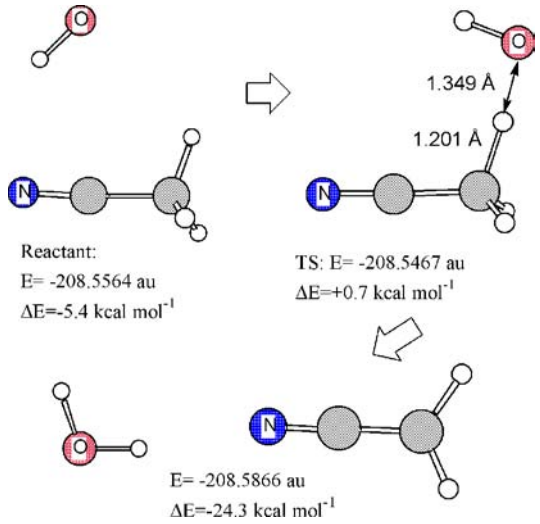

Figure 5. Structure and energy change for the reaction $CH_3CN + •OH \rightarrow •CH_2CN + H_2O$.

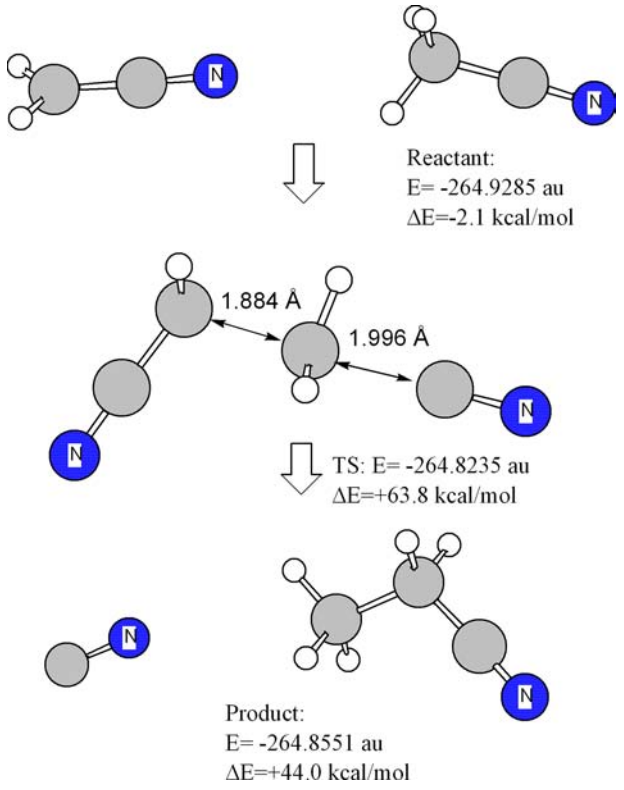

Figure 6. Structure and energy change for the reaction $CH_3CN + •CH_2CN \rightarrow •CN + CH_3CH_2CN$.

further consistent with the observation that CH_3OH is not detected. Finally, the radical coupling of Au with •CN proceeds in a downhill reaction (step 5) that is in good agreement with the *in situ* EPR analysis.

On the basis of the experimental observations and DFT calculations, several elemental steps of the AuCN formation are put together, as illustrated in Scheme 1. In the first stage, •OH radicals (or other ROS) are generated in solution through UV-assisted autoxidation of benzaldehyde (step 1), which is normal in photochemical reactions. Then H abstraction from MeCN produces $•CH_2CN$ radical (step 2). Combination of $•CH_2CN$

dx.doi.org/10.1021/ja305198p | J. Am. Chem. Soc. 2012, 134, 18286−18294

Scheme 1. Tentative Reaction Mechanism for the Photosynthesis of AuCN from the AuNP/CH_3CN/benzaldehyde Ternary System in Open Air under UV Irradiation

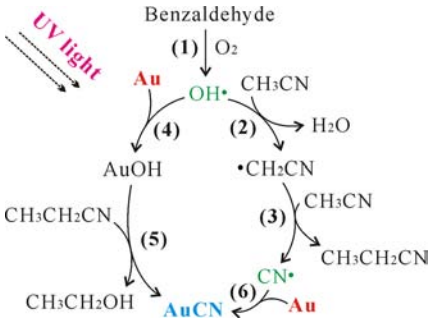

radical with another MeCN molecule, and subsequent C−C bond fission in •[$NC-CH_3CH_2CN$], generates cyanogen derivatives (e.g., CH_3CH_2CN) and •CN radical (step 3). In addition, as a possible side reaction, the resulting CH_3CH_2CN molecules would be transformed into CH_3CH_2OH and AuCN *via* a putative AuOH intermediate (steps 4 and 5). Finally, the whole process is ceased by termination reactions in which •CN collides and combines with Au atoms to produce AuCN (step 6). Regarding the whole photosynthesis, it is recommended that the core reaction is definitely the •CN radical attack on AuNPs to give rise to AuCN, leaving the formation of AuOH and CH_3CH_2OH nonessential, though these side reactions might be, for some reason, unavoidable. In brief, the stoichiometry of overall reactions is described as follows:

$$4CH_3CN + 3\bullet OH + 3Au \rightarrow CH_3CH_2CN + CH_3CH_2OH + 3AuCN + 2H_2O \quad (4)$$

It should be noted that the exact reaction pathway is still an open question due to the difficulty in quantitative determination of the reaction products, but the radical nature of the photoreaction system has been confirmed. Although the oxidation of AuNPs has been sporadically reported,[36] for example, Liz-Marzán and co-workers have shown an interesting spatially directed oxidation of AuNPs by Au(III)−CTAB complexes,[37] our present strategy is different from theirs, especially considering the involvement of •CN radicals. By using this photosynthetic pathway, AuCN oligomers have been successfully fabricated on a variety of supports, as shown in Figure 7. In parallel, other nanosized metal cyanides can also be synthesized from their corresponding zerovalent metals (Figure S7−S13 in the Supporting Information). The methodological universality thus not only offers us a credible way to systematically investigate the interactions between metal cyanides and their supports but also allows us to alter the intrinsic properties (e.g., magnetic, optical, and catalytic properties) of certain metal cyanides by employing different kinds of supports.

3.3. TEM Observations. Although AuCN has particularly simple formulas, it is actually an inorganic polymer that consists of infinite linear Au−CN−Au−CN chains arranged in parallel.[38,39] More importantly, it has been reported that two or more closed-shell Au(I) cations often form aggregates in one-dimensional (1-D) or two-dimensional (2-D) geometry. The significant attractive interaction between Au(I) centers is commonly referred to as "aurophilicity", which is equivalent to

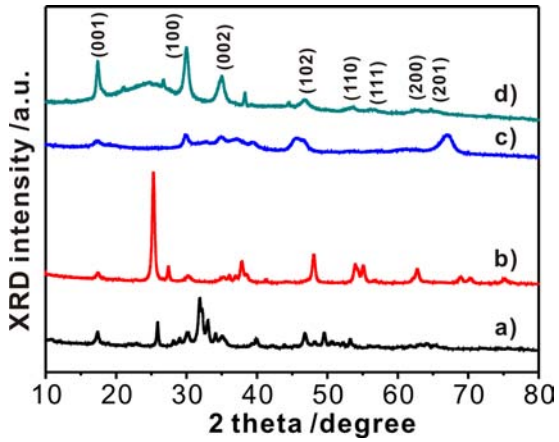

Figure 7. XRD patterns of AuCN oligomers supported on different supports: (a) hydroxyapatite, (b) P25-TiO_2, (c) γ-Al_2O_3, and (d) active carbon.

that of hydrogen bonding.[40] We believe that the radical process will promote the contraction of Au−Au distance, and also the oligomerization of AuCN, as indicated by its unique spectral results (*vide supra*). Therefore, to obtain clear information of the growth property of AuCN is rather meaningful. In this case, mesoporous silica (FDU-12) with ordered ultralarge spherical cages[20] and silica submicrospheres (SiO_2MS) are chosen as two typical supports. The microtomed samples collected at different reaction intervals were used for transmission electron microscopy (TEM) observations.

Figure 8a revealed that the encapsulated AuNPs are homogeneously distributed within the mesoporous networks before the photoreaction, while they became much larger after only 0.5 h of UV irradiation due to Ostwald ripening at harsh reaction environment (Figure 8b). Nevertheless, tiny grains emerged around the bulky AuNPs that exhibit a "satellite-like" structure (cyan circle). These grains are undoubtedly AuCN oligomers owing to the appearance of its corresponding XRD peaks and the remarkable color change (Figure 8b, inset), suggesting that AuNPs are cleaved and oligomerized into AuCN oligomers under the attack of free •CN radicals. The oligomers subsequently diffused into the solution phase and thus separated from each other. As a function of the reaction time, larger AuNPs gradually disappeared and more and more AuCN oligomers with a size of approximately 3.5 nm are found to be confined in the well-defined mesopores (Figure 8c−e with inset showing their corresponding XRD spectra). Interestingly, we also noticed that 2-D AuCN nanorods with lengths of tens of nanometers are located outside the mesostructures (Figure 8f), implying that AuCN oligomers are further polymerized into supramolecular structures if without physical barriers.

To further identify the oligomerization behavior of AuCN, SiO_2MS with favorable external surfaces are promising supports. Figure 9a shows that AuNPs are well dispersed on the smooth surface of SiO_2MS before photoreaction. Similarly, the "satellite-like" analogues are also observed upon photoreaction for 1 h (Figure 9b). Moreover, numerous AuCN oligomers are randomly spread over the SiO_2MS surfaces as the reaction proceeds for another hour, which is ultimately polymerized into enormous oligomers with different sizes and shapes upon longer photoirradiation (Figure 9c,d). It is reasonable that the size and shape variety of AuCN oligomers

dx.doi.org/10.1021/ja305198p | J. Am. Chem. Soc. 2012, 134, 18286−18294

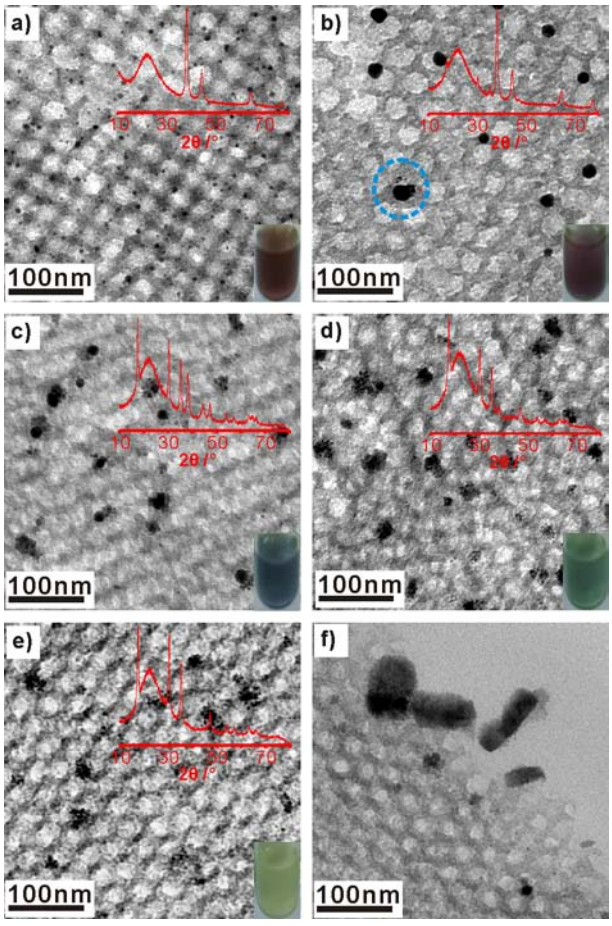

Figure 8. TEM images of AuNPs/FDU-12 before (a) and after (b) 0.5 h, (c) 1 h, (d) 1.5 h, and (e) 2 h of photoreaction (the inset is the corresponding XRD spectrum and photographs), and (f) AuCN nanorods are formed on the edge of the support.

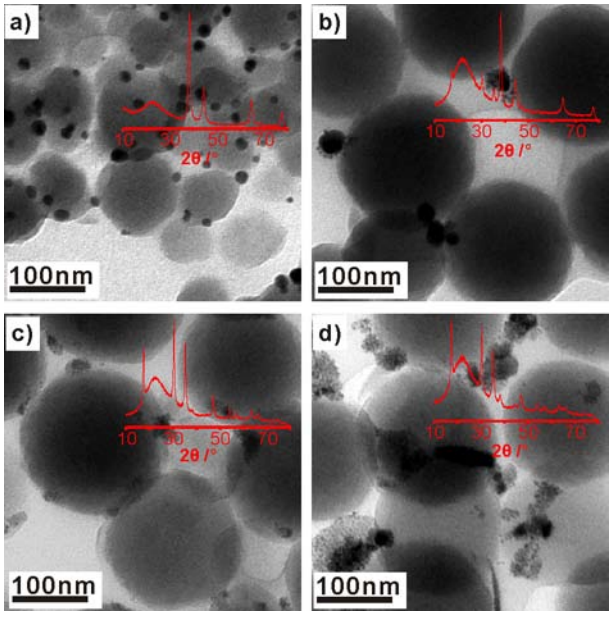

Figure 9. TEM images of AuNP/SiO_2 submicrospheres before (a) and after (b) 1 h, (c) 2 h, and (d) 4 h of photoreaction (the inset is the corresponding XRD spectrum).

allow its unique spectroscopic response in comparison with previous reports.[21,23] Importantly, the structural complexity as well as the d^{10} Au(I) ions enable the supported AuCN oligomers to be harnessed to develop effective heterogeneous/homogeneous catalysts, optical/magnetic nanodevices,[41,42] and therapeutic nanomedicine[43] based on Au(I) chemistry.

3.4. Catalytic Applications. In order to further demonstrate the existence of AuCN oligomers, Au(I) catalysis employing AuCN as the active species seems to be a useful tool. Herein, we described the homogeneous AuCN/PBu_3-catalyzed annulation of salicylaldehyde with phenylacetylene to give isoflavanone that is valuable in the synthesis of isoflavanone-type natural products (Table 2).[17] This annulation

Table 2. Supported AuCN Oligomers and PBu_3 Catalyzed Annulation of Salicylaldehyde with Phenylacetylene to Give Isoflavanone[a]

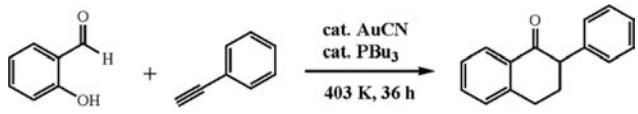

entry	cat. (mol %)	PBu_3 (mol %)	t (h)	T (K)	yield (%)
1	0.33	8.33	36	363	0
2	0.33	8.33	36	383	<1
3	0.33	8.33	36	403	6.9
4	0.33	8.33	36	423	7.4
5	0.33	8.33	12	403	1.7
6	0.33	8.33	24	403	5.1
7	0.33	8.33	48	403	8.0
8	1	5	36	403	0
9	1	10	36	403	<1
10	1	25	36	403	11.1
11	1	50	36	403	11.3
12	4	100	36	403	47.6
13	0.33	0	36	403	0
14	0	8.33	36	403	1.5
15[b]	0.33	8.33	36	403	0
16[c]	0.33	8.33	36	403	2.1
17[d]	4	100	36	403	38.2
18[e]	4	100	36	403	26.9
19[f]	4	100	36	403	32.1
20[g]	4	100	36	403	42.5

[a]Mesoporous silica is used as the support from entries 1 to 16; isoflavanone was purified and obtained after the following reaction: 5 mL of salicylaldehyde, 0.11 mL of phenylacetylene, 29.7 mg of supported AuCN (5.0 wt %), and 0.083 mL of PBu_3 in distilled toluene were mixed and stirred in a sealed reactor at 403 K under nitrogen for 36 h. [b]Mesoporous silica supported AgCN. [c]Mesoporous silica supported AuNPs instead of AuCN were used as the catalysts. [d]SiO_2MS was used as the support for AuCN oligomers. [e]MgO was used as the support for AuCN oligomers. [f]TiO_2 (Degussa P25) was used as the support for AuCN oligomers. [g]Hydroxyapatite was used as the support for AuCN oligomers.

incorporates all atoms in both starting materials into the product and thus has a theoretical atom economy of 100%. The best conditions found, which led to the isolation of isoflavanone in 47.6% yield, were the use of 4 mol % of an AuCN source (5 wt % AuCN supported on mesoporous silica) and 100 mol % of PBu_3 (Table 2, entry 12). AuCN or PBu_3 alone provided none or only a trace amount of the desired product (Table 2, entries 13 and 14, respectively). When the alternative catalysts AgCN and AuNPs were used, the yield of the product

dx.doi.org/10.1021/ja305198p | J. Am. Chem. Soc. 2012, 134, 18286−18294

decreased rapidly to 0 and 2.1%, respectively (Table 2, entries 15 and 16, respectively), indicating the unique catalytic property of AuCN for such C−C bond formation reaction. Notably, relatively good yield is obtained at a lower temperature (403 K) as compared to previous work (423 K),[17] which is supposed to be caused by the size effect of our nanoparticulate catalysts. It is well accepted that, in gold catalysis, the catalytic properties of AuNPs largely depend on their supports.[44−46] However, it is still an open question whether Au(I) catalysis follows this rule. Obviously, the versatility of the present radical pathway potentially allows us to improve the catalytic properties of AuCN by using different kinds of supports. Primary results showed that mesoporous silica is the best support for AuCN oligomers to catalyze the annulation transformation (Table 2, entries 12 and 17−20), which is possibly ascribed to the confinement effect of mesopores. However, it is difficult to suppress the diffusion of active AuCN/PBu_3 species into the reaction solution due to the homogeneous character of the reaction and the large entrance size of mesoporous silica (∼10 nm). Therefore, the engineering of the entrance size (less than 2 nm) is a possible way to encapsulate or immobilize the active catalytic species within the porous structure and prevent their leaching problem, as evidenced in the case of heterogenization of homogeneous chiral catalysts in SBA-16.[47] Additionally, Corma and co-workers have reported that cationic Au(III) species can be stabilized on CeO_2 and ZrO_2 rather than on silica and carbon.[48] It is thus expected that large-scale screening of the supports to find an optimal one is able to turn the current Au(I) based homogeneous system into heterogeneous with possibility. Accordingly, further works on gaining insights into the reaction mechanism using different metal sources and supports and their applications for both homogeneous and heterogeneous catalysis are now underway in our laboratory.

4. CONCLUSIONS

In summary, we have developed a radical-involved photochemical cyanidation strategy to prepare AuCN oligomers using metallic AuNPs and MeCN as precursors, which is proved to be one-pot, mild, universal, and green. The synthetic system is of potential significance and engineering value for metallurgy, organometallic chemistry, metal cyanide nanoparticles synthesis, and recycling of noble metals. During the photosynthesis, the activation and transformation of the C−C bond of MeCN is fascinating. In addition, this work has much fundamental importance to the gold chemistry: (i) AuNPs are photochemically oxidized by free radicals to directly produce AuCN oligomers which could be useful in other cyanation processes in organic syntheses. (ii) The free radical oligomerization of solid-state AuCN is demonstrated, and the AuCN oligomers possess unusual spectral properties that may result from the well-known "aurophilicity" and their special 1-D geometry. (iii) Supported AuCN can catalyze certain C−C bond formation reactions that is of benefit to the development of Au(I) catalysis.

■ ASSOCIATED CONTENT

Supporting Information

Synthesis of materials; material characterization; EPR experiments; ^{1}H NMR results; DFT calculations; XRD patterns of various supported metal cyanides; and TEM images of monodispersed AuNPs, AgNPs, PtNPs, PdNPs, and RuNPs. This material is available free of charge via the Internet at http://pubs.acs.org.

■ AUTHOR INFORMATION

Corresponding Author

jfan@zju.edu.cn

Present Address

[‖]Shanghai Institute of Organic Chemistry, Chinese Academy of Sciences, Shanghai, China.

Notes

The authors declare no competing financial interest.

■ ACKNOWLEDGMENTS

We acknowledge helpful discussions with Prof. L. M. Zhang at UCSB and Prof. Y. H. Zhang at ZJU. This work was supported by the National Science Foundation of China (20873122, 21222307, and 21003106), Fok Ying Tung Education Foundation (131015), and the Fundamental Research Funds for the Central Universities (2012QNA3014).

■ REFERENCES

(1) Johnson, J. C. F. *Getting Gold a Practical Treatise for Prospectors, Miners and Students with Illustrations*; British Library, Historical Print Editions: Exeter Street, Strand, London, U.K., 2011.

(2) Pyykko, P. *Angew. Chem., Int. Ed.* **2004**, *43*, 4412−4456.

(3) Rubo, A.; Kellens, R.; Reddy, J.; Steier, N.; Hasenpusch, W. *Ullmann's Encyclopedia of Industrial Chemistry*; Wiley-VCH Verlag GmbH & Co. KGaA: Boschstrasse 12, D-69469 Weinheim, Germany, 2000.

(4) Wang, X.-B.; Wang, Y.-L.; Yang, J.; Xing, X.-P.; Li, J.; Wang, L.-S. *J. Am. Chem. Soc.* **2009**, *131*, 16368−16370.

(5) Urban, V.; Pretsch, T.; Hartl, H. *Angew. Chem., Int. Ed.* **2005**, *44*, 2794−2797.

(6) Oyama, S. T.; Gaudet, J.; Zhang, W.; Su, D. S.; Bando, K. K. *ChemCatChem* **2010**, *2*, 1582−1586.

(7) Jacobs, M. B.; Jagodzinski, P. W.; Jones, T. E.; Eberhart, M. E. *J. Phys. Chem. C* **2011**, *115*, 24115−24122.

(8) Katz, M. J.; Ramnial, T.; Yu, H. Z.; Leznoff, D. B. *J. Am. Chem. Soc.* **2008**, *130*, 10662−10673.

(9) Ling, Y.; Chen, Z. X.; Zhou, Y. M.; Weng, L. H.; Zhao, D. Y. *CrystEngComm* **2011**, *13*, 1504−1508.

(10) Marlin, D. S.; Olmstead, M. M.; Mascharak, P. K. *Angew. Chem., Int. Ed.* **2001**, *40*, 4752−4754.

(11) Reniers, G.; Brebbia, C. A. Sustainable Chemistry; *Computational Mechanics*WIT press: Ashurst Lodge, Ashurst, Southampton SO40 7AA, U.K., 2007.

(12) Hirata, Y.; Yada, A.; Morita, E.; Nakao, Y.; Hiyama, T.; Ohashi, M.; Ogoshi, S. *J. Am. Chem. Soc.* **2010**, *132*, 10070−10077.

(13) Grochowski, M. R.; Li, T.; Brennessel, W. W.; Jones, W. D. *J. Am. Chem. Soc.* **2010**, *132*, 12412−12421.

(14) Ochiai, M.; Hashimoto, H.; Tobita, H. *Angew. Chem., Int. Ed.* **2007**, *46*, 8192−8194.

(15) Jiang, Z.; Huang, Q.; Chen, S.; Long, L.; Zhou, X. *Adv. Synth. Catal.* **2012**, *354*, 589−592.

(16) *The Flavonoids: advances in research*; Harborne, J. B., Mabry, T. J., Eds.; Chapman and Hall: London, New York, 1982.

(17) Skouta, R.; Li, C.-J. *Angew. Chem., Int. Ed.* **2007**, *46*, 1117−1119.

(18) Wei, C.; Li, C.-J. *J. Am. Chem. Soc.* **2003**, *125*, 9584−9585.

(19) Gorin, D. J.; Sherry, B. D.; Toste, F. D. *Chem. Rev.* **2008**, *108*, 3351−3378.

(20) Ma, G.; Yan, X.; Li, Y.; Xiao, L.; Huang, Z.; Lu, Y.; Fan, J. *J. Am. Chem. Soc.* **2010**, *132*, 9596−9597.

(21) Rawashdeh-Omary, M. A.; Omary, M. A.; Patterson, H. H. *J. Am. Chem. Soc.* **2000**, *122*, 10371−10380.

(22) Assefa, Z.; McBurnett, B. G.; Staples, R. J.; Fackler, J. P.; Assmann, B.; Angermaier, K.; Schmidbaur, H. *Inorg. Chem.* **1995**, *34*, 75−83.
(23) Leung, K. H.; Phillips, D. L.; Tse, M. C.; Che, C. M.; Miskowski, V. M. *J. Am. Chem. Soc.* **1999**, *121*, 4799−4803.
(24) Cho, K.; Jang, Y. S.; Gong, M. S.; Kim, K.; Joo, S. W. *Appl. Spectrosc.* **2002**, *56*, 1147−1151.
(25) Bal, B. C. *Autoxidation*; International Book Marketing Service Ltd: Mauritius, Africa, 2011.
(26) Stan, S. D.; Daeschel, M. A. *J. Agric. Food Chem.* **2005**, *53*, 4906−4910.
(27) Zalomaeva, O. V.; Trukhan, N. N.; Ivanchikova, I. D.; Panchenko, A. A.; Roduner, E.; Talsi, E. P.; Sorokin, A. B.; Rogov, V. A.; Kholdeeva, O. A. *J. Mol. Catal. A: Chem.* **2007**, *277*, 185−192.
(28) Molinari, A.; Montoncello, M.; Rezala, H.; Maldotti, A. *Photochem. Photobiol. Sci.* **2009**, *8*, 613−619.
(29) Chen, Y. R.; Sturgeon, B. E.; Gunther, M. R.; Mason, R. P. *J. Biol. Chem.* **1999**, *274*, 24611−24616.
(30) Reinke, L. A.; Moore, D. R.; Kotake, Y. *Anal. Biochem.* **1996**, *243*, 8−14.
(31) Miyajima, T.; Kotake, Y. *Free Radical Biol. Med.* **1997**, *22*, 463−470.
(32) Rehorek, D.; Salvetter, J.; Hantschmann, A.; Hennig, H.; Stasicka, Z.; Chodkowska, A. *Inorg. Chim. Acta* **1979**, *37*, L471−L472.
(33) Namyatov, I. G.; Babushok, V. I. *Combust., Explos. Shock Waves* **1996**, *32*, 270−275.
(34) Nowicka, A. M.; Hasse, U.; Hermes, M.; Scholz, F. *Angew. Chem., Int. Ed.* **2010**, *49*, 1061−1063.
(35) Chen, G. Z. *Angew. Chem., Int. Ed.* **2010**, *49*, 5413−5415.
(36) Sa, J.; Goguet, A.; Taylor, S. F. R.; Tiruvalam, R.; Kiely, C. J.; Nachtegaal, M.; Hutchings, G. J.; Hardacre, C. *Angew. Chem., Int. Ed.* **2011**, *50*, 8912−8916.
(37) Rodriguez-Fernandez, J.; Perez-Juste, J.; Mulvaney, P.; Liz-Marzan, L. M. *J. Phys. Chem. B* **2005**, *109*, 14257−14261.
(38) Hibble, S. J.; Hannon, A. C.; Cheyne, S. M. *Inorg. Chem.* **2003**, *42*, 4724−4730.
(39) Bowmaker, G. A.; Kennedy, B. J.; Reid, J. C. *Inorg. Chem.* **1998**, *37*, 3968−3974.
(40) Bachman, R. E.; Fioritto, M. S.; Fetics, S. K.; Cocker, T. M. *J. Am. Chem. Soc.* **2001**, *123*, 5376−5377.
(41) Bayse, C. A.; Brewster, T. P.; Pike, R. D. *Inorg. Chem.* **2009**, *48*, 174−182.
(42) Lefebvre, J.; Callaghan, F.; Katz, M. J.; Sonier, J. E.; Leznoff, D. B. *Chem.—Eur. J.* **2006**, *12*, 6748−6761.
(43) Shaw, C. F. *Chem. Rev.* **1999**, *99*, 2589−2600.
(44) Haruta, M.; Yamada, N.; Kobayashi, T.; Iijima, S. *J. Catal.* **1989**, *115*, 301−309.
(45) Comotti, M.; Li, W. C.; Spliethoff, B.; Schuth, F. *J. Am. Chem. Soc.* **2006**, *128*, 917−924.
(46) Haruta, M.; Tsubota, S.; Kobayashi, T.; Kageyama, H.; Genet, M. J.; Delmon, B. *J. Catal.* **1993**, *144*, 175−192.
(47) Yang, H.; Li, J.; Yang, J.; Liu, Z.; Yang, Q.; Li, C. *Chem. Commun.* **2007**, 1086−1088.
(48) Zhang, X.; Corma, A. *Angew. Chem., Int. Ed.* **2008**, *47*, 4358−4361.